

2D speckle tracking imaging to assess sepsis induced early systolic myocardial dysfunction and its underlying mechanisms

T. LI¹, J.-J. LIU², W.-H. DU¹, X. WANG¹, Z.-Q. CHEN¹, L.-C. ZHANG¹

¹Department of Ultrasound, Daping Hospital and Research Institute of Surgery, Military Medical University, Chongqing, China

²Department of Ultrasound, Xiangyang Hospital, Hubei University of Medicine, Xiangyang, Hubei, China

Tao Li and Juanjuan Liu contributed equally to this work

Abstract. – OBJECTIVE: The aim of this study was to apply speckle tracking imaging (STI) to evaluate rabbit sepsis induced myocardial injury.

MATERIALS AND METHODS: Rabbits were injected with the endotoxin lipopolysaccharide (LPS) before and 2h, 4h, 6h, 8h, 12h after the injection of LPS, conventional echocardiography and STI were performed to measure left ventricular end diastolic diameter (LVDd), end-systolic diameter (LVDs), cardiac output (CO), left ventricular ejection fraction (EF), fractional shortening (FS), left ventricular global longitudinal strain (GLS)/GLS rate (GLSr), global circumferential strain/strain rate (GCS/GCSr), and the global radial strain/strain rate (GRS/GRSr). We also observed the injury with optical microscopy. Serum troponin cTnT and TUNEL assays determining myocardial apoptosis were also carried out to determine the induced injury levels.

RESULTS: None of the indicators measured are statistically different in the two groups before the LPS treatment ($p > 0.05$). 2h after LPS injection, in LPS treated group, only GLS/GLSr, GCS/GCSr significantly reduced compared to the control group ($p < 0.05$). 6h, 8h, 12h after LPS injection, EF and FS were lower ($p < 0.05$), LVDd and LVDs were higher ($p < 0.05$), and GLS/GLSr, GCS/GCSr, GRS/GRSr were significantly lower ($p < 0.05$). LPS significantly elevated serum cTnT level in the experimental group ($p < 0.05$). In the LPS treated group, we found pathological changes of the myocardium.

CONCLUSIONS: STI is more sensitive than the conventional echocardiography for the early detection of abnormal myocardial contractility. It is a noninvasive, accurate and timely detection of myocardial dysfunction in sepsis.

Key Words:

Speckle tracking imaging, Sepsis, Myocardial contractile function.

Introduction

Sepsis is a clinical syndrome caused mainly by acute microcirculatory dysfunction, and often occurs in severe trauma, infections, burns, shock or other stress conditions. This leads to bacterial translocation, which is a source of endotoxin. Even in the early, intensive anti-infection treatment, fluid resuscitation and other related organ function support, the overall mortality rate remains as high as 50%¹. Clinical studies confirmed that myocardial dysfunction is the major clinical manifestation of severe sepsis. About 40% of cases of sepsis were associated with cardiac dysfunction, and the severity is highly correlated to the probability of death². Clinically, sepsis has two stages of progression which show differently in hemodynamics: (1) high output stage when cardiac output is normal or higher, and the blood pressure is normal or lower³; (2) low output stage, when the output drops and vascular resistance is increased to compensate, which leads to inadequate blood supply to multiple organs, and eventual organ failure⁴. The myocardial contractile function is often suppressed in sepsis, with reversible dilatation of the left and right ventricular chambers, and reduced ejection fraction. Numerous studies have indicated that cardiac dysfunction exists in the high output stage of sepsis⁵. Although at this stage cardiac output in patients with sepsis can be normal or significantly increased, there exists myocardial dysfunction, with left and right ventricular dilatation and possibly falling systolic function and ventricular compliance. Echocardiography is often combined with an invasive cardiac catheter and pulmonary artery catheters to monitor hemodynamic

changes of patients with sepsis in real-time. Indicators such as left ventricular ejection fraction (LVEF), left ventricular fraction shortening (LVFS) and cardiac output (CO), stroke volume (SV) are heavily influenced by the preload and the afterload. Meanwhile the chamber volume and vascular resistance change significantly in patients with sepsis. Thus, the indicators only serve to evaluate the internal function of cardiac pumping and part of the cardiac muscle. No indicator showing the degree of dysfunction which is not under the influence of the preload and the afterload has yet been found.

2D speckle tracking (STI) is a new ultrasound imaging technique. STI observes the myocardial tissue at many pixels, or the natural acoustic markers in a two-dimensional ultrasound image. These pixels are distributed evenly in the cardiac muscle and are stable acoustic spots. STI imaging recognizes the spot structure on the two-dimensional image and obtains information on the muscle movement or deformation by tracking the structure of these spots. It captures, frame by frame, the change of position of the spot, or relative position between points in the cardiac cycle, and quantitatively computes the variables describing the movements along the axis, radial direction, tangential direction or chamber torsion. It depends less on the cardiac overload, the size of the chamber and the geometrical shape of the heart, compared to an echocardiogram. STI has a higher resolution, both in time and space, to acutely reflect the local systolic and diastolic movements during a cardiac cycle. It enables us to distinguish tiny deformations between different segments of muscles in different time frames. It also helps to evaluate the myocardial function as a whole, and reduces the variance of observations by different observers. Hence, it enhances the reliance of the evaluation result of cardiac function.

Materials and Methods

Animal Models and Grouping

36 healthy rabbits, both male and female, weight 2.25-2.35 kg (Daping Hospital, Third Military Medical University, Institute of Surgery Experimental Animal Center) were randomly categorized into two groups: 18 in experimental group, 18 in the control group. Both groups underwent neck and chest hair removal, right jugular vein cannulation, blood draw and rehydration.

The right femoral artery was cannulated for mean arterial pressure (MAP) monitoring. Endotracheal intubation connected the ventilator tester to monitor the respiratory rate. Electrocardiogram monitoring was used to record the heart rate. The endotoxin LPS (lipopolysaccharide, Sigma, source *Escherichia coli* O111: B4) was injected at the dose of 0.8 mg/kg of body weight. in a 0.04 mg/ml saline solution. The solution was injected slowly into the ear vein with a micropump at the rate of 0.42 ml/min and the injection took 2hrs. For the control, 20 ml per kg of body weight of saline was injected for 2hrs.

Instruments and Methods

Echocardiogram

MyLab30 ultrasound system was applied with a PA122 probe, frequency 7.5 MHz. Regular 2D Echocardiogram and STI examinations were given prior to, and 2h, 4h, 6h, 8h, 12h after LPS injection. Left ventricular end-diastolic diameter (LVDD), left ventricular end-systolic diameter (LVDS) and left ventricular ejection fraction (LVEF) were measured by Simpson's method, cardiac output (CO), left ventricular fractional shortening (LVFS) were measured 3 times by M-mode ultrasound and an average was taken. The short axis view of the left ventricle at the level of papillary muscle and apical four-chamber view were used, and images were captured in three consecutive cardiac cycles. Video data was saved for further off-line analysis. STI quantitative analysis was performed on the Software station MyLab Desk. Cardiac cycles with clear images were selected from the video data and the endocardial region was outlined manually at the end-systolic phase. The region of interest (ROI) was adjusted to match the outline of the endocardium. The epicardial border was generated by the software. Outline of epicardium and endocardium was aligned manually so that the thickness of ROI matched the actual thickness of cardiac muscle. Then, the program was run and the software performed an automatic STI analysis by segmenting the cardiac muscle, which were divided in the long axis and short axis views, into 6 segments. The average of the maximum systolic longitudinal strain/strain rate from the longitudinal strain curve of apical four chamber view was taken as the global longitudinal strain/strain rate (GLS/GLSr) of the left ventricle. Similarly, the global circumferential strain/strain rate (GCS/

GCSr) and the global radial strain/strain rate (GRS/GRSr) was obtained from the corresponding curve of short axis view of papillary muscle (Figure 1).

Optical Microscopy

Six animals were sacrificed for heart samples following blood sampling at 6h, 8h, and 12h after injection of LPS the chest was opened whilst the animal was sedated by ear vein injection of 3% pentobarbital anesthesia, according to 1 ml/kg. We obtained cross-sectional tissue from the the left ventricular short-axis papillary muscle, which was fixed in 10% formalin for forty hours. Tissue was then dehydrated by immersion in 75%, 95%, 100% ethanol then set in paraffin.

Paraffin block of tissue were cut into 8 μm sections and then dried at a constant temperature of 45°C for 45 minute. Slides were stained with hemtoxylin-eosin staining and tissue was visualized with; an Olympus optical microscope BX41 to observe the change on the microscopic structure of the myocardial tissue.

Serum Troponin (cTnT) Detection

3 ml of blood was drawn from the jugular vein 2h, 4h, 6h, 8h, 12h after LPS or saline injection. Blood was centrifuged at 1000-1300 g for 3-5 minutes to separate the serum for further tests. An immunoassay analyzer (Roche, Basel, Switzerland, Cobas e601) was used to quantify the cardiac troponin (cTnT) concentrations.

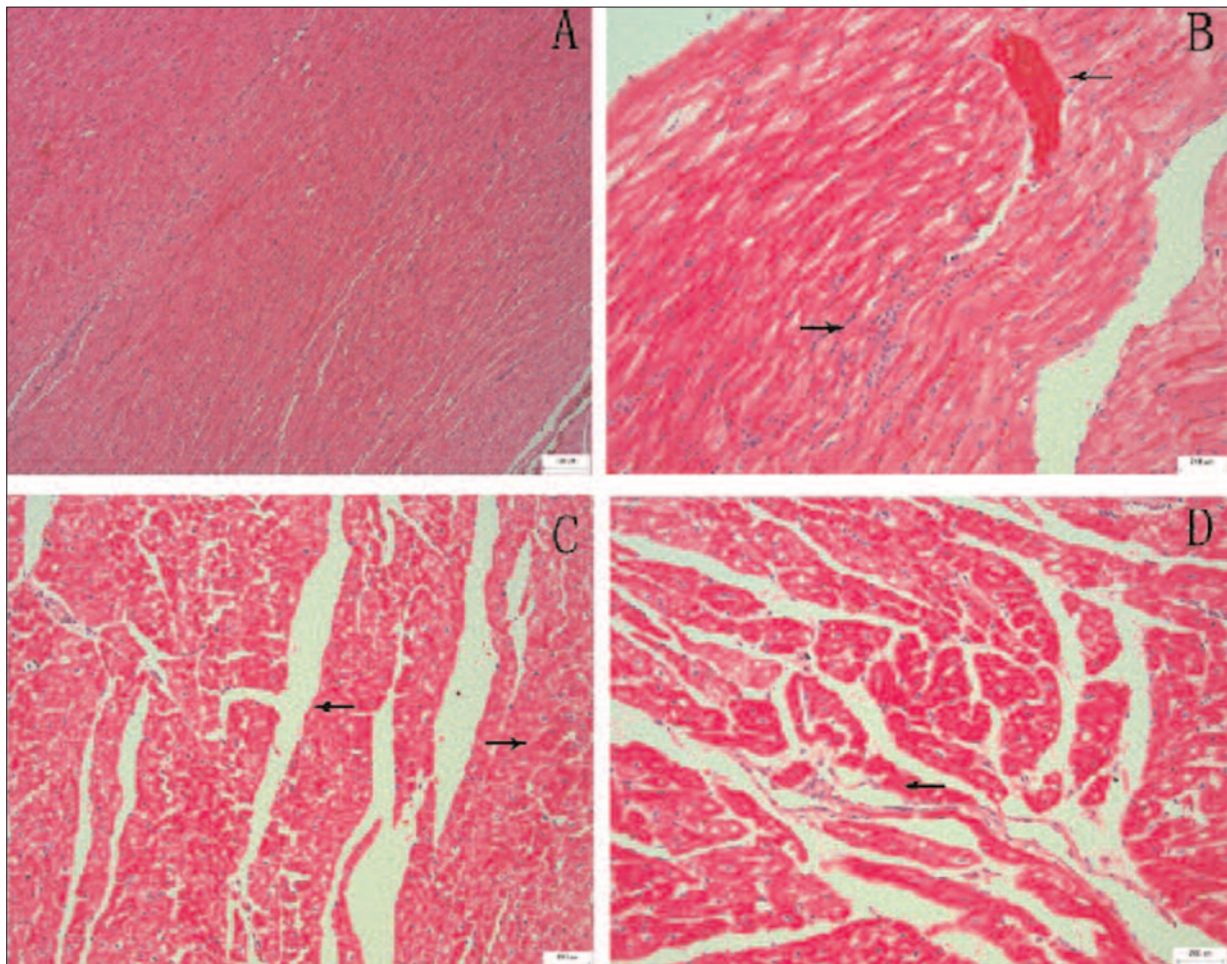


Figure 1. Optical microscopy. **A**, Control Group: Cardiac tissue was intact, with cells well aligned and in healthy shape. No abnormalities of interstitial matrices or microvessel were observed (HE \times 100). **B**, 6h after LPS injections, congestions and hemorrhage occurred in the interstitial tissue (\leftarrow) (HE \times 200). **C**, 8h after LPS injections, cells were unattached. Cell alignment was disorganised and tissue integrity was damaged. Interstitial space was widened and granular degeneration could be seen (\leftarrow) (HE \times 200). **D**, 12h after LPS injections, Interstitial space was widened. Cell orientation was disordered. Granular degeneration, interstitial edema, interstitial congestion, hemorrhage and inflammatory cell infiltration were all observed (\leftarrow) (HE \times 200).

TUNEL Staining

Myocardial tissue samples were fixed in 10% formalin and cut into slices of 20 µm with a cryostat. Slices were washed in phosphate buffered saline (PBS) (2 × 10 min) before being placed in PBS containing 0.1% Triton X-100 and incubated on ice for 2 minutes and again washed in PBS (3 × 10 min). 50 µl of the TUNEL reaction mixture was added for 60 min incubation in darkness at 37°C. then washed in PBS (3 × 10 min). Antifade mounting medium was added and the mounted sample visualised with a fluorescent microscope. Stained cells were counted under five selected views of high magnifications and the average was calculated.

Statistical Analysis

Statistical analysis was performed on SPSS13.0 statistical software (SPSS Inc., Chicago, IL, USA). All quantitative data are presented as mean ± standard deviation. Comparison between two groups were performed using *t* test. Comparison between the parameters was carried out by Pearson correlation coefficient test. A *p* value < 0.05 indicates a statistical significance.

Results

Changes in Vital Signs

2hrs after LPS injection, MAP decreased significantly in the treated group when compared to control group (*p* < 0.05). 6hrs after LPS injection, respiratory rate (RR) and heart rate (HR) increased significantly (*p* < 0.05) (Table I). These signs match the hemodynamics observed at the high output stage of sepsis.

Echocardiogram

Echocardiographic indicators were not significantly different between groups before treatments (*p* > 0.05). 2h after the injection, LPS did not affect LVDD, LVDs, LVEF or LVFS (*p* > 0.05). GLS/GLSr and GCS/GCSr were significantly reduced compared with the control group (*p* < 0.05). GRS/GRSr was not affected (*p* > 0.05). 6h, 8h, 12h after LPS injection, LVEF and LVFS significantly decreased in the treated group (*p* < 0.05). LVDD and LVDs were significantly elevated in the treated group (*p* < 0.05). GLS/GLSr, GCS/GCSr and GRS/GRSr significantly reduced in treated rabbits compared to the control group (*p* < 0.05). CO did not differ significantly between the two groups before or after the treatment (*p* > 0.05) (Table II).

Optical Microscopy

In the control animals, the myocytes were in healthy shape and were well aligned. The interstitial matrix and microvessels had no pathological changes. In contrast, in the treated group myocytes were seen to be not well oriented. The intercellular space was increased and we observed granules present in the myocytes of the treated group, these are a sign of cellular degradation. Interstitial edema, vascular congestion, hemorrhage and inflammatory cell infiltration were also observed (Figure 1).

Change in Serum cTnT

Serum levels of cTnT in treated rabbits rose from 2 hours after LPS injection and continue to increase gradually for the other time points measured, reaching a peak at 12h after LPS injection (Figure 3, Table III).

Table I. Changes in HR, RR and MAP after drug administration ($\bar{x} \pm s$).

	Prior to LPS injection (n=18)	LPS2h (n=18)	LPS4h (n=18)	LPS6h (n=18)	LPS8h (n=12)	LPS12h (n=6)
LPS group						
RR (beats/min)	51 ± 4.4	56 ± 7.97	54 ± 5.35	77 ± 3.55*	78 ± 3.14*	80 ± 1.75*
HR (beats/min)	249 ± 8.27	256 ± 16.91	253 ± 6.9	265 ± 8.3*	272 ± 3.77*	275 ± 4.77*
MAP (KPa)	13.41 ± 0.72	12.5 ± 0.45*	12.49 ± 0.39*	12.78 ± 0.48*	11.92 ± 0.38*	11.78 ± 0.26
Control						
RR (beats/min)	49 ± 4.62	52 ± 4.01	53 ± 4.79	53 ± 4.58	52 ± 3.12	52 ± 3.2
HR (beats/min)	249 ± 8.24	248 ± 7.9	248 ± 7.69	248 ± 7.49	246 ± 6.83	247 ± 8.59
MAP (KPa)	13.31 ± 0.57	13.24 ± 0.57	13.23 ± 0.54	13.46 ± 0.44	13.5 ± 0.58	13.52 ± 0.43

Respiratory rate (RR) and Heart rate (HR) in LPS Group were faster than the Control Group since LPS6h. Mean arterial pressure (MAP) was lower from the injection at 2h. These results match the hemodynamics observed at the high output stage of sepsis. *Compared to the control (*p* < 0.05).

Table II. Comparison of echocardiographic indicators between groups before and after the LPS injection ($\bar{x} \pm s$).

	Prior to LPS	LPS2H (n=18)	LPS4H (n=18)	LPS 6H (n=18)	LPS8H (n=12)	LPS12H (n=6)
Treatment group						
GLS (%)	-13.06 ± 3.06	-9.21 ± 1.47*	-8.71 ± 1.69*	-8.27 ± 1.83*	-8.15 ± 1.04*	-7.26 ± 0.97*
GLSr (1/s)	-1.72 ± 0.34	-1.14 ± 0.20*	-0.96 ± 0.20*	-0.95 ± 0.34*	-0.98 ± 0.27*	-0.88 ± 0.23*
GCS (%)	-8.86 ± 1.51	-7.85 ± 0.87*	-8.81 ± 1.13*	-6.70 ± 0.91*	-7.20 ± 1.14*	-6.97 ± 1.52*
GCSr (1/s)	-1.32 ± 0.14	-1.04 ± 0.11*	-1.26 ± 0.22*	-0.70 ± 0.07*	-0.85 ± 0.04*	-0.83 ± 0.21*
RS (%)	10.79 ± 2.14	9.80 ± 2.44	9.86 ± 0.77	8.13 ± 0.85*	7.24 ± 0.97*	6.75 ± 1.31*
GRSr (1/S)	1.33 ± 0.38	1.38 ± 0.36	1.42 ± 0.14	1.06 ± 0.20*	0.98 ± 0.23*	0.91 ± 0.21*
LVEF (%)	80.0 ± 2.61	79.0 ± 1.41	79.17 ± 2.32	70.83 ± 3.43*	68.17 ± 2.48*	64.17 ± 2.64*
LVFS (%)	44.33 ± 2.94	43.0 ± 1.41	43.0 ± 2.09	37.67 ± 2.42*	35.17 ± 3.13*	32.83 ± 3.06*
LVDD (mm)	10.27 ± 0.53	9.43 ± 0.78	10.98 ± 0.94	11.58 ± 0.93*	11.38 ± 0.94*	12.18 ± 1.00*
LVDS (mm)	5.67 ± 0.40	5.45 ± 0.55	6.27 ± 0.58	7.23 ± 0.71*	7.39 ± 0.77*	8.17 ± 0.59*
CO (L/min)	0.20 ± 0.02	0.21 ± 0.03	0.22 ± 0.02	0.21 ± 0.01	0.21 ± 0.02	0.20 ± 0.02
Control group						
GLS (%)	-12.72 ± 1.55	-12.06 ± 1.94	-11.20 ± 1.45	-10.99 ± 1.01	-11.12 ± 1.06	-11.05 ± 1.39
GLSr (1/s)	-1.54 ± 0.17	-1.60 ± 0.20	-1.19 ± 0.07	-1.35 ± 0.24	-1.51 ± 0.41	-1.40 ± 0.49
GCS (%)	-9.29 ± 1.01	-9.89 ± 1.98	-11.15 ± 1.70	-9.05 ± 0.72	-9.53 ± 0.51	-9.25 ± 0.89
GCSr (1/s)	-1.31 ± 0.17	-1.34 ± 0.27	-1.71 ± 0.34	-1.22 ± 0.13	-1.33 ± 0.08	-1.35 ± 0.16
GRS (%)	10.37 ± 1.84	10.24 ± 1.84	10.41 ± 2.22	10.46 ± 0.86	9.97 ± 1.17	9.29 ± 1.12
GRSr (1/s)	1.46 ± 0.51	1.40 ± 0.18	1.27 ± 0.25	1.45 ± 0.32	1.26 ± 0.15	1.44 ± 0.32
LVEF (%)	80.0 ± 2.28	78.67 ± 2.42	79.33 ± 2.33	78.67 ± 1.63	79.33 ± 2.16	79.00 ± 1.41
LVFS (%)	44.33 ± 2.33	43.0 ± 2.37	43.83 ± 1.94	43.17 ± 1.94	43.67 ± 1.51	43.33 ± 1.97
LVDD (mm)	10.27 ± 0.83	10.21 ± 0.60	10.67 ± 0.46	10.50 ± 0.58	10.28 ± 0.63	10.55 ± 0.52
LVDS (mm)	5.63 ± 0.37	5.82 ± 0.27	6.0 ± 0.35	5.97 ± 0.38	5.79 ± 0.37	5.97 ± 0.27
CO (L/min)	0.20 ± 0.02	0.20 ± 0.02	0.20 ± 0.01	0.21 ± 0.03	0.20 ± 0.02	0.20 ± 0.01

*Compared to the control ($p < 0.05$). GRS/GRSr: Global radial strain/strain rate; LVDD: left ventricular end-diastolic diameter; LVDS: left ventricular end-systolic diameter; CO: cardiac output. 2h after LPS injection, in LPS treated group, only global longitudinal strain/strain rate (GLS/GLSr) and global circumferential strain/strain rate (GCS/GCSr) were significantly reduced compared to the control group ($p < 0.05$). 6h, 8h, 12h after LPS injection, left ventricular ejection fraction (LVEF) and left ventricular fraction shortening (LVFS) were lower ($p < 0.05$), left ventricular end-diastolic diameter (LVDD) and left ventricular end-systolic diameter (LVDS) were higher ($p < 0.05$), and GLS/GLSr, GCS/GCSr, GRS/GRSr were significantly lower ($p < 0.05$).

Correlation Analysis Between cTnT and STI Indicators

The STI indicators GLS, GLSr, GCS, GCSr, GRS, GRSr were all significantly correlated to the level of cTnT, with GLS and GLSr having the highest correlations with cTnT ($r = 0.52$, $r = 0.51$), this suggests that reduction of the strain/strain rate is consistent with the severity of myocardial injury, and GLS, GCSr is more accurate, more sensitive in reflecting the degree of myocardial damage (Table IV).

TUNEL Assay

Minimal apoptosis was present in the control group (green fluorescent spots). However, the level of apoptosis was markedly increased in the treatment group, as shown by the dense green fluorescent 6h, 8h, 12h after the injection of LPS (Table V, Figure 2).

Discussion

Animal Model

It was reported that employing a low-dose (e.g. 1 mg/kg) of LPS can induce high output sepsis in rabbit and, significantly higher doses (e.g. 5 mg/kg) have a profound myocardial depressant effect, leading to sudden acute heart failure (cardiovascular collapse)⁶. A prolonged continuous injection of low dose LPS best simulates the constant release of endotoxin into the blood and thoroughly elicits inflammatory reactions⁷. By sustaining a high cardiac output and a low vascular resistance, researchers can produce animals with pathological conditions highly similar to those of patients with sepsis. In our investigation, we adopted the constant injection of low dose LPS method to produce an animal model that possessed the hemodynamic features of high output sepsis, such as unaffected CO and HR, significantly increased RR and attenuated MAP.

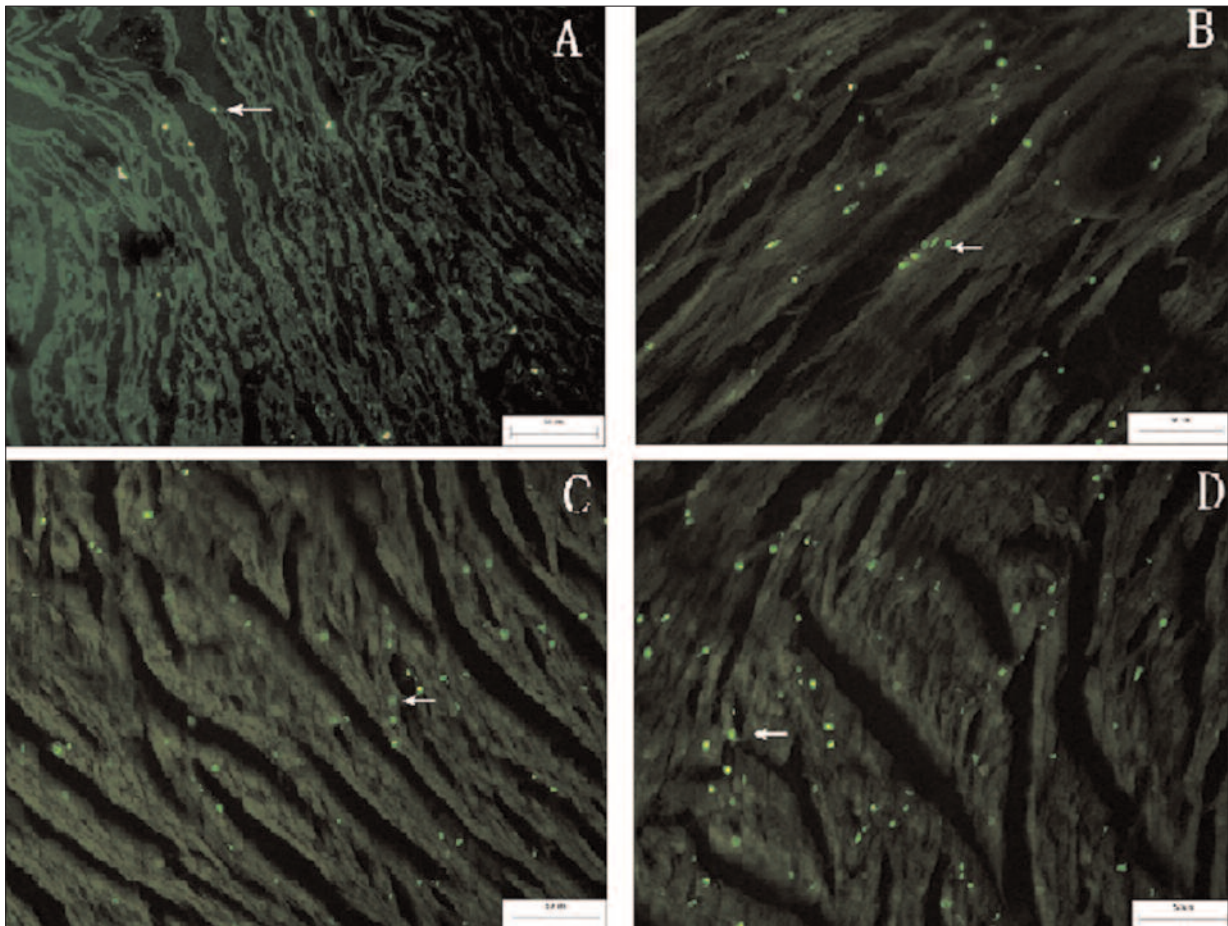


Figure 2. Measure of Apoptosis. TUNEL assays were used to measure the level of apoptosis in the tissue. Fluorescent green spots signify apoptotic cells (\leftarrow) in **A**, Control Group. **B**, 6h after LPS treatment. **C**, 8h after LPS treatment. **D**, 12h after LPS treatment ($\times 400$).

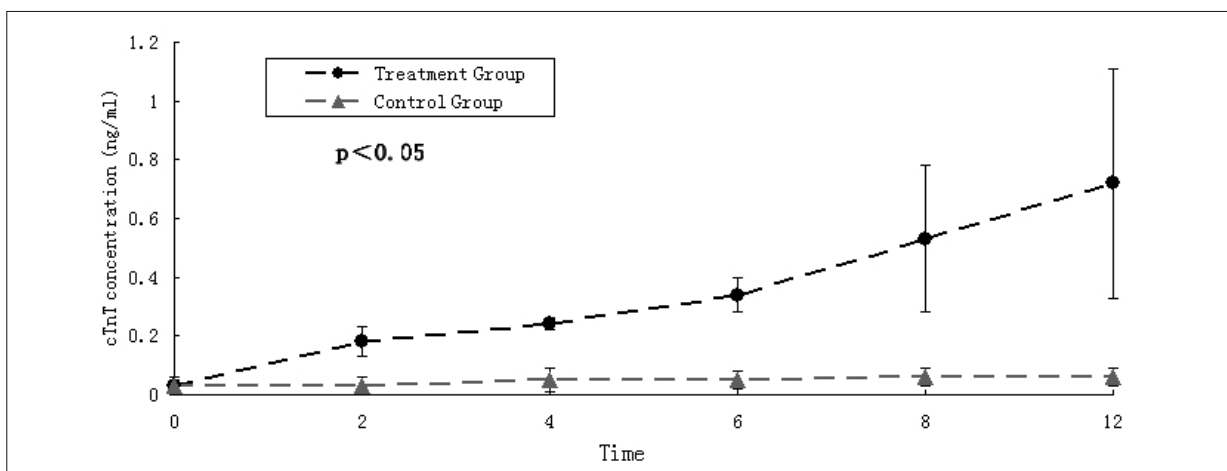


Figure 3. **A**, **B**, Change regulation of cTnT over time. Serum cTnT level in the experimental group gradually increase, from LPS 2h, and reached a peak at 12h after LPS injection ($p < 0.05$). *Indicates a significant difference from the control with a p value < 0.05 .

Table III. Changes in cTnT ($\bar{x} \pm s$).

	Prior to LPS (n=18)	LPS2H (n=18)	LPS4H (n=18)	LPS6H (n=18)	LPS8H (n=12)	LPS12H (n=6)
Treatment group	0.03 ± 0.02	0.18 ± 0.05*	0.24 ± 0.02*	0.34 ± 0.06*	0.53 ± 0.25*	0.72 ± 0.39*
Control group	0.03 ± 0.03	0.03 ± 0.03	0.05 ± 0.04	0.05 ± 0.03	0.06 ± 0.03	0.06 ± 0.03

Table IV. Correlation analysis of myocardial injury marker cTnT to STI indices.

	GLS	GLSr	GCS	GCSr	GRS	GRSr
cTnT <i>r</i>	0.52	0.51	0.506	0.505	0.496	0.493
<i>p</i>	0.001	0.001	0.002	0.002	0.002	0.002

The correlation coefficient, *r* means whether there is a linear relationship between the two variables, and the strength of the linear relationship is positive or negative correlation. *p* used to test the truth of relationship between the two variables. It is statistical significance with a *p* value < 0.05. GLS/GLSr, GCS/GCSr, GRS/GRSr have good correlation with cTnT, and GLS/GLSr have the strongest correlation.

Table V. Apoptotic cell counts before and after treatment ($\bar{x} \pm s$).

	Prior to LPS injection	LPS 6H	LPS8H	LPS12H
Treatment group	6 ± 1.94	32 ± 5.2	37 ± 7.12	44 ± 6.56
Control group	6 ± 1.72	6 ± 1.09*	6 ± 1.47*	6 ± 1.63*

*Indicates a significant difference from the control with a *p* value < 0.05.

Ultrasound Assessment of Myocardial Contractile Function

Rabbit cardiac muscles contain fibers going in three different directions: longitudinally, helically, and in rings. These fibers are fundamental to the various deformations that the heart can undergo. STI recognizes the myocardial deformation from different directions, and can distinguish not only longitudinal motions, but also circumferential and radial motions. Thus, it detects early abnormal deformations⁸. Many articles have recorded the application of STI to the diagnosis of heart diseases. Sengupta SP⁹ found in subclinical hypertensive patients with normal left ventricular systolic function, that both the LS of both endocardium and epicardium and the CS of subepicardial muscles were significantly lower than the control. However, RS was unchanged in those patients. This showed that STI has the advantage to detect cardiac abnormalities even at the stage of subclinical hypertension. STI also contributes to the understanding of ongoing changes in mus-

cle fibers so as to maintain normal LVEF and LVFS. Donal et al¹⁰ showed in a pig model of aortic coarctation using STI, that LS dropped significantly in the low level of aortic coarctation, while the RS remained unchanged in the intermediate level of aortic coarctation. In another report¹¹, it was demonstrated that in pigs with cardiac ischemia induced by atherosclerosis, LS and CS were more sensitive than RS in showing the local functional changes in cardiac muscles, caused by ischemia. Li et al¹² developed a dog model with acute heart failure, by intravenous injection of propofol and esmolol. They found that LS/LSr and CS/CSr could identify abnormal deformations on the longitudinal axis and short axis of the left ventricle despite of a normal LVEF. Basu et al¹³ employed STI to assess the left ventricular contractile functions of 15 cases of pediatric septic shock, in which the conventional echocardiogram failed to identify any abnormalities. However the STI results showed a reduction in both LS/LSr and CS/CSr. These indices were

independent of volume expansion therapy and vasodilating drugs, which can interfere with the cardiac loading. After the application of agents that enhance cardiac contractility, the FS and EF returned to normal. However, the strain/strain rate indices remained lower than normal. We found that 2h and 4h after the LPS, the blood pressure of the rabbit began to drop and the heart rate did not change. In other words, blood pressure post-injection was reduced to sustain a normal contractile function. With conventional echo indices LVDs, LVDD, LVEF and LVFS remained unchanged. This taken with reduced left ventricular GLS/GLSr and GCS/GCSr, leads us to believe that the internal contractility of cardiac muscle was attenuated. All the results stated above suggested the existence of cardiac impairments during subclinical sepsis, even when LVEF and LVFS showed no pathological alteration. The contractile function of left ventricle needs normal fibers oriented in different directions to sustain the global systolic function. Keeping GRS/GRSr on a normal level is an important way of compensation for normal LVEF after GLS/GLSr and GCS/GCSr drop. LPS injections led to LVDs and LVDD greater than the control at 6h, 8h and 12h post-injection. However, LVEF and LVFS were significantly lower than that in the control group. When the LVEF and LVFS go down, by Frank–Starling’s law, the left ventricular volume will increase and the heart will beat faster to maintain normal CO. At this time, all STI indices GLS/GLSr, GCS/GCSr and GRS/GRSr will drop. This means that as sepsis worsens, and the cardiac injury develops further. In spite of the compensating mechanism to maintain cardiac output, the general contractility of the heart is significantly weakened. We showed that these strains and strain rates are correlated to the heart impairment marker in serum cTnT. In particular, GLS and GLSr highly related to the serum cTnT level. This meant the degree of changes in STI indices reflect the degree of cardiac injury, and GLS and GLSr are best among these indices.

Mechanisms of Cardiac Injury

cTnT (cardiac troponin T) is an intracellular protein regulating cardiac muscle contractility. It is also a sensitive and specific marker of cardiac impairment, capable of giving assessment and prognosis of left ventricular function. The serum cTnT level is low under normal physiology.

However, when myocytes are damaged and die, cTnT is released into the blood. A significantly elevated serum cTnT was shown to be attributed to the attenuated stroke work index and lower LVEF in 31%-85% of patients with sepsis in the clinic¹⁴. The precise mechanism of cTnT release and associated cardiac impairment are not clear. Possible pathways include: factors such as bacterial endotoxin exerting direct damage on myocytes; circulating inflammatory mediators or cytokines such as tumor necrosis factor (TNF- α), interleukin (IL-1 β), complement component C5a that have toxic effects on the cardiac cells; oxidation injury where NO reacts with superoxide anion O₂⁻ to become NO₃⁻, and is further processed into reactive oxygen species (ROS) which denature protein, disrupt Ca²⁺ flow, inhibit mitochondrial respiration, suppress respiratory chain, damages mitochondrial membrane lipid and destroy transmembrane enzyme activity on mitochondria membrane¹⁵. Microcirculation dysfunction, as endotoxin induces the vascular endothelial cells to express a variety of adhesion molecules such as ICAM-1 (intercellular adhesion molecule-1) which promotes neutrophil adherence to the endothelium, which triggers the production of thrombin and the formation of fibrin. As the end result, thrombosis or even disseminated intravascular coagulation (DIC) will interrupt cardiac blood supply, rendering the myocytes in hypoxia and subsequent irreversible damage¹⁶. Endotoxin has injurious effects on myocardium through the pathways stated above, leading to troponin enzymolysis and the leakage of cTnT. Then, high levels cTnT built up in the blood^{17,18}. Rising in serum cTnT level started at 2h after the LPS injection, continued to increase and peaked at 12h. This suggests that LPS was damaging the cardiac muscle through a complicated mechanism, and that the degree of damage increased over time. From the cardiac tissue, we observed disrupted cell attachment, degenerative changes, local vascular congestion, hemorrhage, interstitial edema and inflammatory cell infiltration. These were evidence of damage to the cardiac muscle caused by the endotoxin. Apoptosis is cellular programmed death, which is essential to the development and the homeostasis of tissues. Inflammation, ischemic reperfusion and stress can induce cardiomyocyte apoptosis, damaging to the structural integrity of myocardial tissue and eventually leading to heart failure or cardiac arrhythmias or other severe medical consequences. In our ex-

periments, apoptosis levels were increased by LPS, starting 6h post injection, and continuing to increase thereafter. Apoptosis definitely played a role in the cardiac damage that occurs in sepsis. Our results were consistent with previous reports³¹. Our rabbit model was verified by the fact that we succeeded in reproducing the enhanced cTnT and other pathological changes that are seen in patients with sepsis. Apoptosis and pathological damage to cardiac muscle could be one of the reasons why the cardiac function was reduced in rabbit with sepsis.

Our study shows that in our model, the cardiac output did not change during the high output stage of sepsis, suggesting the cardiac function is normal. Nevertheless, STI indicators GLS, GLSr, GCS and GCSr suggested the opposite, which is consistent with the story that the serum marker cTnT told. This implies that STI is better than the conventional echocardiography in picking up cardiac abnormalities in the high output stage of sepsis. It is a more accurate, reliable and sensitive method for cardiac impair evaluation in the context of sepsis. Pathological damages to the myocytes and the interstitial matrices could be one of the reasons behind falling heart function in sepsis.

Conclusions

In the current study, we evaluated the sepsis-induced myocardial injury in rabbit models using light microscopy, serum troponin cTnT, conventional echocardiography, and STI. As demonstrated by the results of the TUNEL assays, cell apoptosis was involved in the pathogenesis of sepsis-induced myocardial injury. Conventional echocardiography and 2D STI showed that both the myocardial motion and the cardiac functions were damaged, although to different extents, in the rabbit sepsis models. The STI parameters, including GLS, GLSr, GCS, and GCSr STI, in combination, were more sensitive than the conventional echocardiography for the early detection of abnormal myocardial contractility. In addition, the STI findings were highly correlated with cTnT. Therefore, STI is a noninvasive, accurate, and timely approach for detecting sepsis-induced myocardial dysfunction.

Conflict of Interest

The Authors declare that there are no conflicts of interest.

Acknowledgements

This study was supported by the Chongqing Science and Technology Project (Grant No. CSTC2012jjB10034), and Natural Science Foundation of China (Grant No. 81271586).

References

- 1) DOMBROVSKIY VY, MARTIN AA, SUNDERRAM J, PAZ HL. Rapid increase in hospitalization and mortality rates for severe sepsis in the United States: a trend analysis from 1993 to 2003. *Crit Care Med* 2007; 35: 1244-1250.
- 2) SOLOMKIN JS, MAZUSKI J. Intra-abdominal sepsis: Newer interventional and antimicrobial therapies. *Infect Dis Clin North Am* 2009; 23: 593-608.
- 3) KUMAR A, HAERY C, PARRILLO JE. Myocardial dysfunction in septic shock. *Crit Care Clin* 2000; 16: 251-287.
- 4) HOESEL LM, NIEDERBICHLER AD, WARD PA. Complement-mediated molecular events in sepsis leading to heart failure. *Mol Immunol* 2007; 44: 95-102.
- 5) HOLLENBERG SM, DUMASIU A, EASINGTON C, COLILLA SA, NEUMANN A PARRILLO JE. Characterization of a hyperdynamic murine model of resuscitated sepsis using echocardiography. *Am Respir Crit Care Med* 2001; 164: 891-859.
- 6) LEVY RJ, DEUTSCHMAN CS. Evaluating myocardial depression in sepsis shock. *Shock* 2004; 22: 1-10.
- 7) COPELAND S, WARREN HS, LOWRY SF, CALVANO SE, REMICK D. Acute inflammatory response to endotoxin in mice and human. *Clin Diagn Lab Immunol* 2005; 12: 60-67.
- 8) WANG ZHOU, LI JIAN, REN YONGFENG, ZHU TIANGANG. Study progress and application of two-dimensional strain echocardiography. *Chinese J Medial Imaging Technol* 2008; 24: 959-962.
- 9) SENGUPTA SP. Early impairment of left ventricular function in patients with systemic hypertension: new insights with 2-dimensional speckle tracking echocardiography. *Indian Heart J* 2013; 65: 48-52.
- 10) DONAL E, BERGEROT C, THIBAUT H, ERNANDE L, LOUFOUA J, AUGÉUL L, OVIZE M, DERUMEUX G. Influence of afterload on left ventricular radial and longitudinal systolic functions: A two-dimensional strain imaging study. *Eur J Echocardiogr* 2009; 10: 914-921.
- 11) FU Q, XIE M, WANG J, WANG X, LV Q, LU X, FANG L, CHANG L. Assessment of regional left ventricular myocardial function in rats after acute occlusion of left anterior descending artery by two-di-

- mensional speckle tracking imaging. *J Huazhong Univ Sci Technolog Med Sci* 2009; 29: 786-790.
- 12) LI C, LI T, ZHANG J, WU W, ZHU D, DIAN K, RAO L. Performance of echocardiographic parameters in sequential monitoring of left ventricular function in an animal model of acute heart failure. *Echocardiography* 2010; 27: 1274-1281.
 - 13) BASU S, FRANK LH, FENTON KE, SABLE CA, LEVY RJ, BERGER JT. Two-dimensional speckle tracking imaging detects impaired myocardial performance in children with septic shock, not recognized by conventional echocardiography. *Pediatr Crit Care Med* 2012; 13: 259-264.
 - 14) VER ELST KM, SPAPEN HD, NAM NGUYEN D, GARBAR C, HUYGHENS LP, GORUS FK. Cardiac troponins I and T are biological markers of left ventricular dysfunction in septic shock. *Clin Chem* 2000; 46: 650-657.
 - 15) FLYNN A, CHOKKALINGAM MANI B, MATHER PJ. Sepsis-induced cardiomyopathy: a review of pathophysiologic mechanisms. *Heart Fail Rev* 2010; 15: 605-611.
 - 16) MERX MW, WEBER C. Sepsis and the heart. *Circulation* 2007; 116: 793-802.
 - 17) VER ELST KM, SPAPEN HD, NGUYEN DN, GARBAR C, HUYGHENS LP, GORUS FK. Cardiac troponins I and T are biological markers of left ventricular dysfunction in septic shock. *Clin Chem* 2000; 46: 650-657.
 - 18) MEHTA MJ, KHAN IA, GUPTA V, JANI K, GOWDA RM, SMITH PR. Cardiac troponin I predicts myocardial dysfunction and adverse outcome in septic shock. *Int J Cardiol* 2004; 95: 13-17.